Canadian Science Publishing

ARTICLE

Trends in phytoplankton communities within large marine ecosystems diverge from the global ocean

Kevin D. Friedland, John R. Moisan, Aurore A. Maureaud, Damian C. Brady, Andrew J. Davies, Steven J. Bograd, Reg A. Watson, and Yannick Rousseau

Abstract: Large marine ecosystems (LMEs) are highly productive regions of the world ocean under anthropogenic pressures; we analyzed trends in sea surface temperature (SST), cloud fraction (CF), and chlorophyll concentration (CHL) over the period 1998–2019. Trends in these parameters within LMEs diverged from the world ocean. SST and CF inside LMEs increased at greater rates inside LMEs, whereas CHL decreased at a greater rates. CHL declined in 86% of all LMEs and of those trends, 70% were statistically significant. Complementary analyses suggest phytoplankton functional types within LMEs have also diverged from those characteristic of the world ocean, most notably, the contribution of diatoms and dinoflagellates, which have declined within LMEs. LMEs appear to be warming rapidly and receiving less solar radiation than the world ocean, which may be contributing to changes at the base of the food chain. Despite increased fishing effort, fishery yields in LMEs have not increased, pointing to limitations related to productivity. These changes raise concerns over the stability of these ecosystems and their continued ability to support services to human populations.

Résumé : Les grands écosystèmes marins (LME) sont des régions très productives de l'océan planétaire exposées à des pressions d'origine humaine. Nous analysons les tendances de la température de la surface de la mer (TSM), de la proportion de nuages (PN) et de la concentration de chlorophylle (CHL) durant la période de 1998 à 2019. Les tendances de ces paramètres dans les LME divergent de celles de l'océan planétaire. La TSM et la PN ont augmenté plus rapidement dans les LME, alors que la CHL a diminué plus rapidement. Cette dernière a diminué dans 86 % de tous les LME, 70 % de ces baisses étant statistiquement significatives. Des analyses complémentaires indiqueraient que les types fonctionnels de phytoplancton dans les LME ont également divergé de ceux de l'océan planétaire, notamment en ce qui concerne les contributions des diatomées et des dinoflagellés, qui ont baissé dans les LME. Les LME semblent se réchauffer rapidement et recevoir moins de rayonnement solaire que l'océan planétaire, ce qui pourrait contribuer à des changements à la base de la chaîne alimentaire. Malgré un effort de pêche accru, les rendements des pêches dans les LME n'ont pas augmenté, ce qui indique des limites reliées à la productivité. Ces changements soulèvent des inquiétudes concernant la stabilité de ces écosystèmes et leur capacité de continuer à soutenir des services aux populations humaines. [Traduit par la Rédaction]

Introduction

Seafood production is dependent on multiple factors, not least of which includes the productivity of phytoplankton at the base of marine food webs. Phytoplankton biomass is dynamic, changing seasonally with the timing and intensity of blooms, and subject to shifting climate conditions. A principal factor that can change phytoplankton bloom initiation, duration, and biomass is the shoaling of mixed layer depths due to increasing temperature, which limits vertical mixing (Somavilla et al. 2017) and the redistribution of dissolved nutrients (Henson et al. 2013). Arguably the most prominent aspect of climate change has been the change in thermal regimes on both global and local scales (Cheng et al. 2019). There is growing evidence that the lower trophic levels of marine ecosystems have been responding to climate factors as evidenced by changes in productivity (Roxy et al. 2016), phytoplankton community structure (Dutkiewicz et al. 2019), and bloom phenology (Friedland et al. 2018). While it is anticipated that climate change will alter the vertical structure of the water column, it is worth noting that stratification has already undergone substantial change in recent years (Yamaguchi and Suga 2019).

Hence, it is prudent to examine responsive change in lower trophic levels to these contemporary trends in climate, allowing us to gauge current and near future trajectories of system productivity and the potential for sustained seafood yields.

Received 11 November 2020. Accepted 6 May 2021.

K.D. Friedland. Northeast Fisheries Science Center, Narragansett, Rhode Island, USA.
J.R. Moisan. Wallops Flight Facility, Goddard Space Flight Center, Wallops Island, Virginia, USA.
A.A. Maureaud. Centre for Ocean Life & Section for Ecosystem Based Marine Management, National Institute for Aquatic Sciences (DTU Aqua), Technical University of Denmark, Denmark; Center for Biodiversity & Global Change, Department of Ecology & Evolutionary Biology, Yale University, New Haven, Connecticut, USA.
D.C. Brady. School of Marine Sciences, University of Maine, Walpole, Maine, USA.
A.J. Davies. Department of Biological Sciences, University of Rhode Island, Kingston, Rhode Island, USA.
S.J. Bograd. Environmental Research Division, NOAA Southwest Fisheries Science Center, Monterey, California, USA; Institute of Marine Sciences, University of California-Santa Cruz, Santa Cruz, California, USA.
R.A. Watson and Y. Rousseau. Centre for Marine Socioecology, University of Tasmania, Private Bag 129, Hobart, Australia; Institute for Marine and Antarctic Studies, University of Tasmania, Private Bag 129, Hobart, Australia.

Corresponding author: Kevin D. Friedland (email: kevin.friedland@noaa.gov).

Prior to the development of remote-sensing thermal and ocean color measurement systems, it was difficult to characterize the change in temperature and chlorophyll concentration in marine ecosystems on a global scale. The time series for remote-sensing data have matured and now allow for the simultaneous comparison of multiple parameters for a period of over two decades (Groom et al. 2019). Temperature can influence processes in marine ecosystems at both the individual and system levels; individuals can respond to temperature increases with a change in base metabolism (Dantas et al. 2019) and populations can respond with shifts in trait variation (Salo et al. 2020). Changes at the individual level can then cause marine ecosystems to reorganize as the distributional ranges of species shift and community richness changes, most demonstratively related to temperature change (Batt et al. 2017; Frainer et al. 2017; Burrows et al. 2019). While fishing has historically had the greatest influence on marine ecosystem structure and productivity (Shackell et al. 2012), climate effects are increasingly becoming the dominant forcing factors (Merillet et al. 2020). The availability of longer and richer time series of temperature and fisheries data has likely influenced the development of hypotheses of climate control of marine ecosystem function towards ideas that are largely temperature-centric.

Primary production estimates in marine ecosystems are constrained by seasonal and transient variations in light reaching the ocean surface. The quantity of photosynthetically active radiation (PAR) can vary by an order of magnitude with changing cloud conditions. In the Indian Ocean, measurements of PAR associated with clear skies were in excess of 600 $\mu mol \cdot m^{-2} \cdot s^{-1}$; however, cloudy conditions typically lowered PAR to less than 100 $\mu mol \cdot m^{-2} \cdot s^{-1}$ (Jyothibabu et al. 2018). In Antarctic waters, chlorophyll concentration was found to be correlated with PAR and measured cloud fraction, which demonstrates the light limitation of phytoplankton biomass (La and Park 2016). This effect was most closely associated with mid- and high-level clouds in the study area. Strom et al. (2010) conditioned estimates of water column productivity with cloud cover and pycnocline depth as covariates, and concluded that both had direct effects on light availability and indirect effects on phytoplankton physiology. They noted that cloud cover would likely be an important climate change factor affecting primary production in the Gulf of Alaska. The variation in light level, both the level of solar radiation and the time course of light availability, can play a role in determining the dominant species contributing to seasonal blooms (Joy-Warren et al. 2019). This phenomenon can have important ramifications when diatoms or chlorophyte bloom taxa are replaced by cyanobacteria species given the appropriate light conditions, with obvious implications for food chain transfer of newly fixed carbon. Microplankton such as diatoms are more readily captured by grazing species and facilitate the transfer of energy in marine food webs (Wirtz 2012; Harvey et al. 2019), whereas picoplankton such as cyanobacteria tend to be filtered less efficiently and are often refractory to digestion raising concerns about their effects on food web stability (Ullah et al. 2018).

The overall stability of ecosystems is related to the stability of lower trophic level productivity, which can directly influence the capacity to produce surplus biomass to support fisheries and exert control over the stability of fisheries-related economic systems. Ecosystem stability has been described as a function of energy flow among producers and consumers (Huxel and McCann 1998), and when trophic transfer is inhibited by thermally related factors, new equilibrium among phytoplankton functional groups can be established (Ullah et al. 2018). This can be particularly problematic when groups like cyanobacteria begin to dominate and tend to be a refractory food resource (Friedland et al. 2005); however, some cyanobacteria taxa can also be toxic, which can affect the human consumption of seafood (Paerl 2018). The energy flow in marine ecosystems is event driven by the timing and magnitude of production cycles; hence, phenological mismatches can be of critical importance. The reproductive cycles of many marine species are timed to match seasonal production of blooms to benefit the feeding of early life stages. For example, recruitment success in marine fish can be affected by the timing of seasonal blooms (Asch et al. 2019). Bloom production variability can also affect the growth and reproduction in adult populations by impacting the availability and energy content of forage species (Durant et al. 2019). Perturbations among higher trophic level species affect the diversity and stability of the ecosystem, which often results in a shift in fishery exploitation to lower trophic level taxa, hence exacerbating the problem of system stability maintenance (Howarth et al. 2014). These perturbed ecosystems are often continental shelf large marine ecosystems (Halpern et al. 2007), which are a focus of both global and national food security since the fisheries in large marine ecosystems play a more important role in providing harvestable seafood than high seas fisheries (Schiller et al. 2018).

The aim of this study is to examine contemporary trends in sea surface temperature, cloud fraction, and chlorophyll concentration from remotely sensed data sources for the Global Ocean, with particular focus on large marine ecosystems (LMEs). LMEs are defined according to range of factors, and have come to provide a way to differentiate continental seas from the open ocean (Sherman 1991). LMEs cover approximately 25% of the world's oceans, but generate 80% of global fisheries production (Christensen et al. 2008) and provide on the order of $USD 13 trillion in ecosystem services (Costanza et al. 2014). Trends in lower trophic level indicators are further scrutinized for potential change in dominant phytoplankton functional types (PFT), again contrasting change inside and outside LMEs. Finally, trends in fisheries catches and catch per unit effort (CPUE) are investigated as a potential indicator of integrated change among higher trophic levels to changes in the physical environment and lower trophic levels.

Materials and methods

Remote-sensing data sources

We utilized remote-sensing data from multiple sensors spanning the period 1998–2019 to develop our depiction of physical and biological change globally and within Large Marine Ecosystems. LMEs are global biomes bounded by the coast and the extent of the continental shelf, with each LME generally having distinct bathymetry and hydrography (Sherman and Duda 1999). LMEs have higher productivity and host more diverse biological communities than found in the open ocean (see online Supplementary Fig. S1[1]). Sea surface temperature (SST) data were sourced from the NOAA Optimum Interpolation Sea Surface Temperature Analysis (OISST) dataset version 2.0, which provides high resolution sea surface temperature (Reynolds et al. 2007). SST was examined at a spatial resolution of 1° and temporal resolution of 1 month, which are available from the Physical Sciences Laboratory website (https://psl.noaa.gov/data/gridded/data.noaa.oisst.v2.html). We examined remote sensing parameters available from the Hermes GlobColour website (http://hermes.acri.fr/) including chlorophyll *a* concentration (CHL) and cloud fraction (CF). CHL was based on the Garver, Siegel, Maritorena Model (GSM) merged data product that combines a four-sensor time series (including Sea-viewing Wide Field of View Sensor (SeaWiFS), Moderate Resolution Imaging Spectroradiometer on the Aqua satellite (MODIS), Medium Resolution Imaging Spectrometer (MERIS), and Visible and Infrared Imaging/Radiometer Suite (VIIRS) sensors) using a bio-optical model inversion algorithm (Maritorena et al. 2010). CF was calculated as the percentage of pixels flagged as cloudy and is also a merged data product.

[1]Supplementary data are available with the article at https://doi.org/10.1139/cjfas-2020-0423.

Table 1. Summary of relationship between various phytoplankton types, their range of observed size classes and associated pigments adapted from Jeffrey et al. (2011) and Kramer and Siegel (2019).

	Red algal lineage						Green algal lineage			Cyanobacteria		
	Diatoms	Dinoflagellates	Chrysophytes	Pelagophytes	Haptophytes	Cryptophytes	Prasinophytes	Euglenoids	Chlorophytes	Trichodesmium	Synochococcus	Prochlorococcus
Class size												
Micro	+*	+*	+	–	+	–	–	+*	+	+	+	+
Nano	+	+	+*	+*	+*	+*	+*	+	+*	+	+	+
Pico	–	–	+	+	+	–	+	–	+	+*	+*	+*
Chlorophylls												
MV Chlorophyll *a*	4	4	4	4	4	4	4	4	4	4	4	0
DV Chlorophyll *a*	0	0	0	0	0	0	0	0	0	0	0	5
MV Chlorophyll *b*	0	2	0	0	0	0	4†	4†	4†	0	0	0
DV Chlorophyll *b*	0	0	0	0	0	0	0	0	0	0	0	5†
Chlorophyll *c*12	3	3	4	4	3	3	0	0	0	0	0	0
Chlorophyll *c*3	3	3	0	2	3	0	0	0	0	0	0	0
Xanthophylls												
Alloxanthin	0	1	0	0	0	4†	0	0	0	0	0	0
Diadinoxanthin	4	3	0	4	4	0	0	4	0	0	0	0
Diatoxanthin	3	3	0	3	3	0	0	3	0	0	0	0
Fucoxanthin	4†	3	4	4	4	0	0	0	0	0	0	0
Neoxanthin	0	2	0	0	0	0	4	3	4	0	0	0
Violaxanthin	2	2	4	0	0	0	4	3	4	0	0	0
Zeaxanthin	2	2	4	4	0	0	3	3	3	4†	4†	4†
19′-Butanoyloxy-fuxoxanthin	0	2	0	4	3	0	0	0	0	0	0	0
19′-Hexanoyloxy-fucoxanthin	0	2	0	0	3†	0	0	0	0	0	0	0
Peridinin	0	3†	0	0	0	0	0	0	0	0	0	0
Prasinoxanthin	0	1	0	0	0	0	3	0	0	0	0	0
Lutein	0	0	0	0	0	0	3	0	4	0	0	0

Note: Class size: micro >20μm; nano 2–20μm, pico 0.2–2μm. Numbers associated with pigments denote the level of pigment occurrence within each taxonomic group, (0) not present, (1) trace, (2) rarely present, (3) often present, (4) always present, (5) unique.

*Notes the size class that the group is most prominent within.

†Pigments used in the Hirata et al. (2011) algorithms.

Table 2. Phytoplankton functional type algorithms from Hirata et al. (2011) used in this study.

PFT	Diagnostic pigment	Estimation formula
Diatoms	Fucoxanthin (Fuco)	1.41Fuco/$\sum$DP[a]
Dinoflagellates	Peridinin (Perid)	1.41Perid/$\sum$DP
Green Algae	Chlorophyll *b* (Chl-*b*)	1.01Chl-*b*/$\sum$DP
Prymnesiophytes	19′-Butanoyloxy-fuxoxanthin (But) 19′-Hexanoyloxy-fuxoxanthin (Hex)	(1.27Hex + 0.35But + 0.60Allo)/$\sum$DP
Cyanobacteria	Zeaxanthin (Zea)	0.86Zea/$\sum$DP

[a]$\sum$DP = 1.41Fuco + 1.41Perid + 1.26Hex + 0.6Allo + 0.35But + 1.01Chl-*b* + 0.86Zea = Chl-*a* (Uitz et al. 2006).

Fig. 1. Global trend in sea surface temperature as Theil–Sen slope estimates in units of °C·decade^{-1} for the period 1998–2019. In addition to national boundaries, outline shapes of large marine ecosystems (LMEs) added to the map. Map drawn using "raster" package in R, with the addition of LME outline from shapefile data obtained from www.sciencebase.gov. [Colour online.]

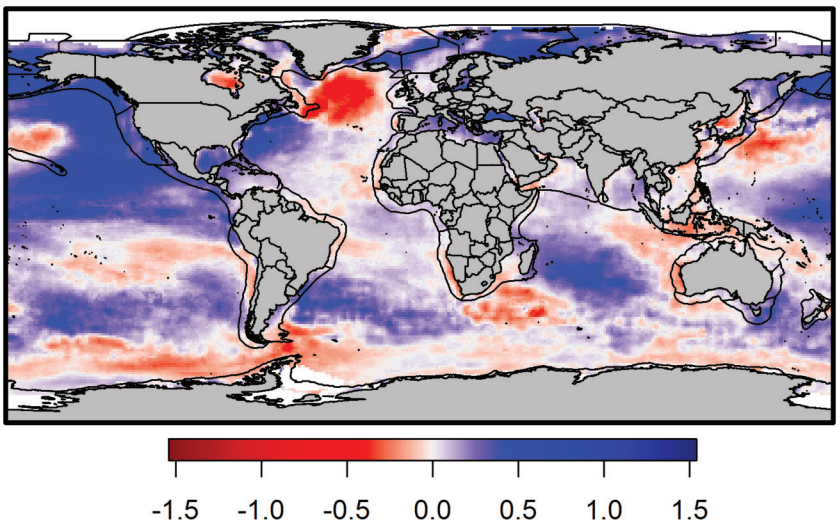

Phytoplankton functional types

The space and time distributions of the PFTs were calculated using a combination of methods developed by Hirata et al. (2011) and Moisan et al. (2017). In the Moisan et al. (2017) study, a satellite-based model for PFTs was developed using pigment measurements from high-performance liquid chromatography (HPLC) analysis and hyperspectral phytoplankton absorption spectra to estimate the pigment-specific absorption spectra for 18 different pigments. The underlying technique involves an inversion using the absorption and pigments at each specific wavelength using singular value decomposition (SVD; Press et al. 1987) to estimate pigment-specific absorption spectra. These spectra were then used with phytoplankton absorption spectra that were modeled as a function of chlorophyll *a* using a simple second-order function. Satellite observations of chlorophyll *a* were then used to estimate the phytoplankton absorption spectra. These estimated spectra, together with the pigment-specific absorption spectra, were used with the non-negative least squares (NNLS; Lawson and Hanson 1995) inversion method to estimate the individual phytoplankton pigment concentrations.

Phytoplankton can be divided into various size classes and functional types based upon their associated pigment compositions. The data in Table 1 were adapted from Kramer and Siegel (2019) using information on size class distributions and pigment associations for various phytoplankton taxa from Jeffrey et al. (2011) and references therein. Estimates of the biomass (percent total chlorophyll *a*) of five PFTs: diatoms, dinoflagellates, green algae, cyanobacteria, and prymnesiophytes, were made using resulting individual phytoplankton pigment concentrations with the PFT formulas of Hirata et al. (2011); see Table 2 for formula specifics.

Strategies to characterize trends

We evaluated the time series changes in temperature using a Mann–Kendall nonparametric test of trend. We calculated Kendall's tau test for the significance (two-tailed test) of a monotonic time series trend (Mann 1945) and calculated Theil-Sen slopes of trend, which is the median slope joining all pairs of observations using the R package "zyp" (version 0.10-1.1). We used the Yue and Pilon method option in that package to estimate Theil-Sen slopes and perform auto-correlation corrected Mann–Kendall tests (Yue et al. 2002). We first calculated the trend for SST, CF, and CHL for the globe on a 1° pixel basis and calculated the means of pixel trends as partitioned by latitude and longitude. We then summarized these trends by computing the mean pixel trend globally and those within the boundaries of LMEs. Next, time series of SST, CF, and CHL for each LME were assembled and trends were tested.

As a precaution to the concern that the trends in CHL in particular may be influenced by strong signals in some subset of the LME data, times series of mean CHL was partitioned by LME with and without significant trends based on the raw data and on the first dimension of a principal component analysis (PCA) of these data groupings. A similar approach was used in the analysis of the PFT data. Trend in PFT was calculated as the change in percent contribution of a PFT over the globe and within and outside LMEs.

Global and large marine ecosystem fishery yields

Global and LME fishery yields were considered from two perspectives, the total catch attributed to world fisheries and measures of CPUE. Fishery removals or total catch data were assembled from the database described in Watson and Tidd (2018). This approach to

Fig. 2. Mean of 1° Theil–Sen slope estimates of sea surface temperature (SST, *a*), cloud fraction (CF, *b*), and chlorophyll concentration (CHL, *c*) as decadal rates over the globe (GLOBE), within large marine ecosystems (IN), and outside large marine ecosystems (OUT) for the period 1998–2019; error bars are 99% confidence intervals. [Colour online.]

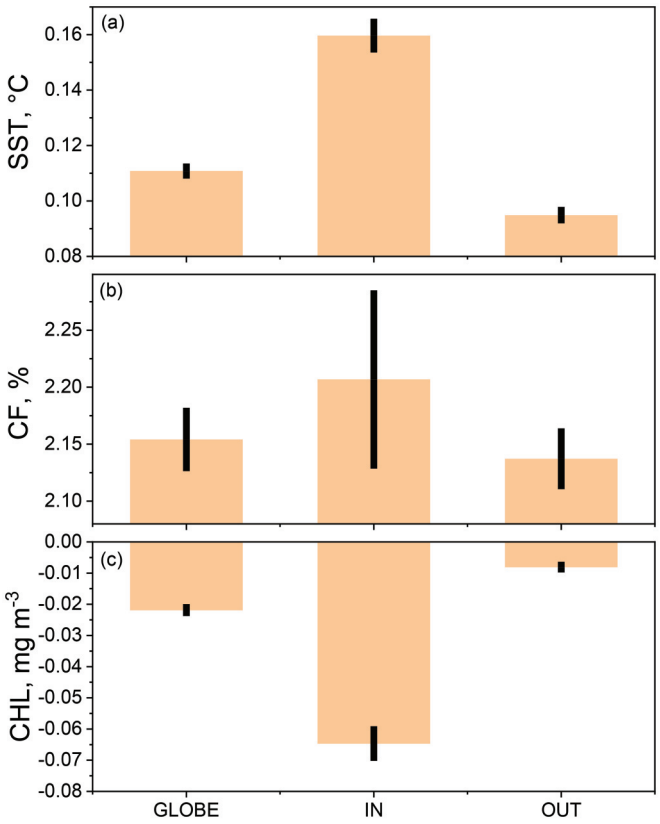

Fig. 3. Mean trends in sea surface temperature (SST, *a*), cloud fraction (CF, *b*), and chlorophyll concentration (CHL, *c*) as decadal rates by latitude for the period 1998–2019. Three values in CHL plot are off scale: 78°S: −0.42; 76°S: −0.31; and 84°N: 0.11. [Colour online.]

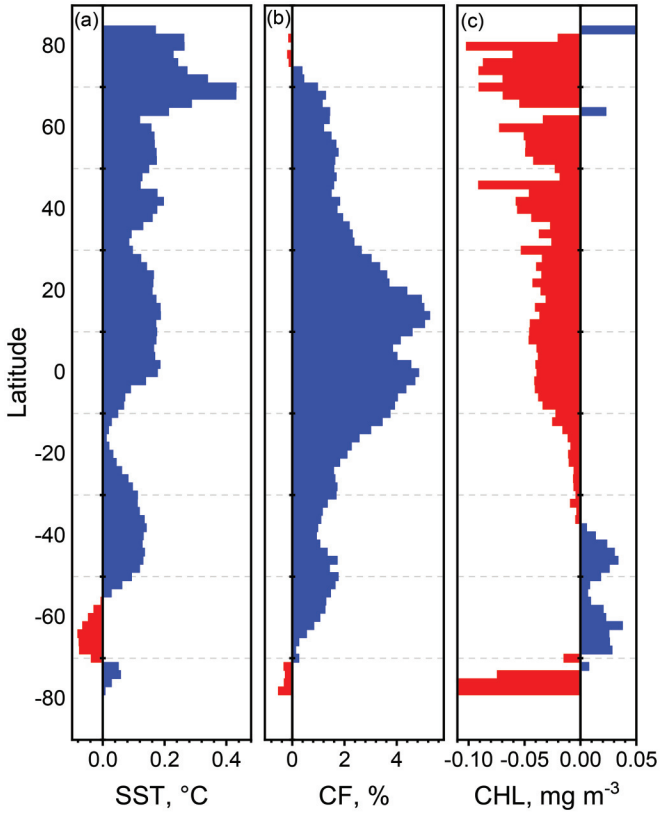

global fisheries sought to harmonize publicly available data and map catches to 0.5° resolution cells guided by the ranges of the reported taxa, inshore fishing arrangements, and satellite data where appropriate. These data include estimates of reported and nonreported catch by fishing sector; however, they do not specifically provide estimates of recreational catch. We examined the trend in global fisheries, and fisheries within and outside LME boundaries during the period nearly matching the extent of the remote sensing data, 1998–2018. We also tested the trends for catch time series of individual LME fisheries. Mapped effective fishing effort by country and sector, adjusted for annual changes in technological efficiency, was based on estimates of vessel numbers and engine power as described in Rousseau et al. (2019). CPUE was defined as the ratio of total catch, including discards and illegal, unreported, and unregulated fishing (IUU), to the total effective effort in an area. As with the catch data, the CPUE time series were also disaggregated between global fisheries and fisheries within and outside LME boundaries; however, the CPUE data were only available over the period 1998–2015. Moreover, as with the catch data, we tested the trends for CPUE time series of individual LME fisheries.

Results

Global patterns of SST, CF and CHL trend

The global pattern of contemporary change in SST revealed distinct differences in the magnitude and direction of thermal shifts by ocean basin over the 22 years of observations. Warming appears most pronounced in the eastern Pacific, western Atlantic, Arctic, and Indian oceans, whereas cooling was evident in the North Atlantic, western Pacific, and Antarctic oceans (Fig. 1). It is important to note that these trends are conditioned on the study period 1998–2019 and will likely vary from other depictions using different time series. The mean of all trend estimates over the globe was approximately 0.11°·decade^{-1}; however, the mean trend within LMEs was approximately 0.16°·decade^{-1} (Fig. 2*a*). Outside of LMEs, the mean trend in SST was less than 0.1°·decade^{-1}. Mean SST trend was positive over all latitudes except a narrow band in the Southern Hemisphere from 56–70 °S (Fig. 3*a*). Similarly, mean SST trend was positive over most longitudes except for two bands of cooling, one associated with the North Atlantic and another in the eastern Indian Ocean (Fig. 4*a*).

Cloud fraction generally increased over most of the globe and in particular over low latitudes. CF increased in excess of 20%·decade^{-1} in some locales and declined at modest rates in Pacific eastern boundary areas, the south Atlantic and Indian oceans (Fig. 5). The global increase in CF averaged 2.15%·decade^{-1} and as with the pattern observed for SST trends, CF trend inside LMEs was greater than the global mean and the trend outside LME was slightly less (Fig. 2*b*). CF trend was positive over most latitudes and trended higher near the equator (Fig. 3*b*). CF trend was positive over all longitudes with the highest rates associated with the region of the Arabian Sea (Fig. 4*b*).

Trend in chlorophyll concentration was more spatially complex than the patterns observed for SST or CF. Both positive and negative trend hot spots appeared within many continental shelf areas (Fig. 6). The global trend in CHL averaged −0.02 mg·m^{-3}·decade^{-1} with the trends inside LMEs averaging some three-fold higher decline or a mean rate less than −0.06 mg·m^{-3} (Fig. 2*c*). CHL trend was mostly negative over latitudes north of 38°S (Fig. 3*c*). CHL trend

Fig. 4. Mean trends in sea surface temperature (SST, *a*), cloud fraction (CF, *b*), and chlorophyll concentration (CHL, *c*) as decadal rates by longitude for the period 1998–2019. [Colour online.]

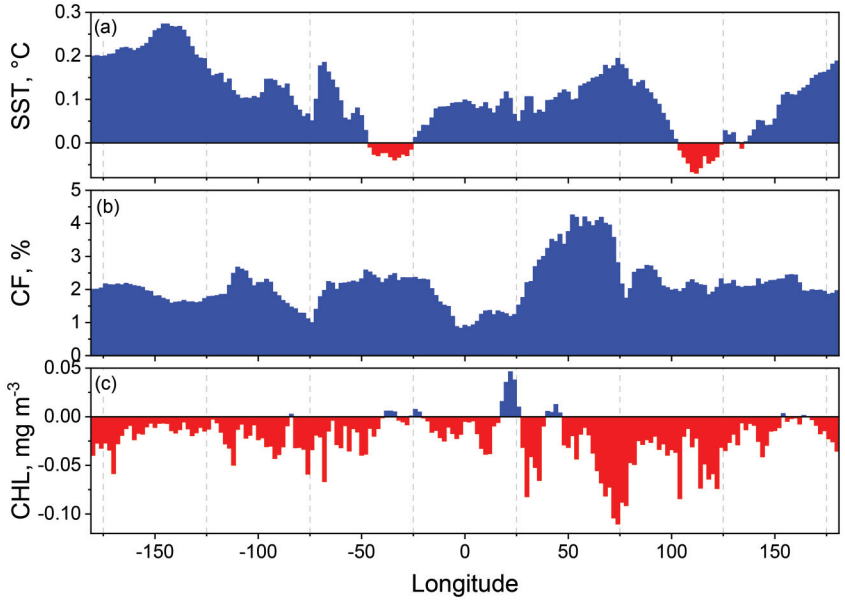

Fig. 5. Global trend in cloud fraction as Theil–Sen slope estimates in units of %·decade^{-1} for the period 1998–2019. In addition to national boundaries, outline shapes of large marine ecosystems (LMEs) added to the map. Map drawn using "raster" package in R, with the addition of LME outline from shapefile data obtained from www.sciencebase.gov. [Colour online.]

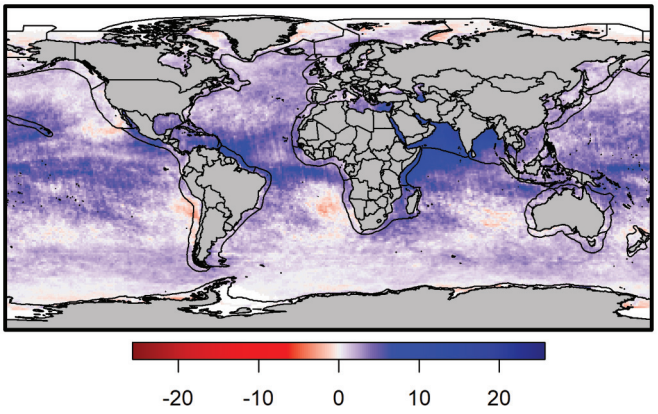

Fig. 6. Global trend in chlorophyll concentration as Theil–Sen slope estimates in unit of mg·m^{-3}·decade^{-1} constrained to ±0.7 for the period 1998–2019. In addition to national boundaries, outline shapes of large marine ecosystems (LMEs) added to the map. Map drawn using "raster" package in R, with the addition of LME outline from shapefile data obtained from www.sciencebase.gov. [Colour online.]

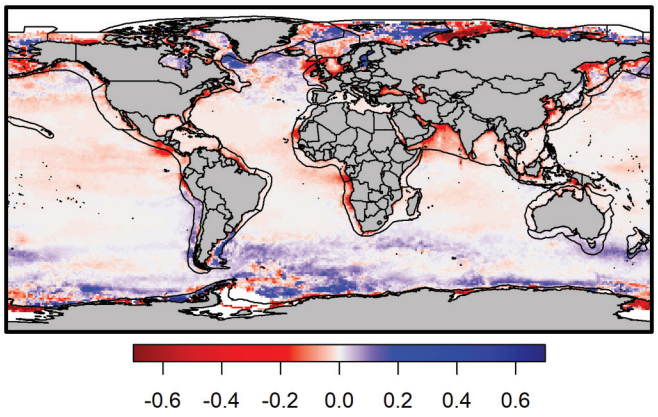

was negative over most longitudes with the highest rates associated with a region of the Indian Ocean (Fig. 4*c*).

To summarize, trends in SST, CF, and CHL in LMEs depart from global mean trends suggesting LME regions are warming more rapidly, experiencing greater cloud cover, and have reduced phytoplankton biomass compared to other parts of the world ocean.

Trends in SST, CF and CHL in individual LMEs

Trends in SST, CF, and CHL within individual LMEs followed the same patterns of change indicated by the mean trends on global scales. The SST in 49 LMEs trended positive, which represents 74% of all LMEs (Table 3 and see Supplementary Table S1[1] for statistics for each LME). Of the SST trends in LMEs, 23 were significant at $p < 0.1$, all of which were positive trends. The trends for CF were even more skewed than the SST trends; 60 or 91% of the individual LME trends were positive. There were 30 significant CF trends by LME, 29 of which were positive trends. As in the

Table 3. Counts of large marine ecosystems (LMEs) with negative and positive Theil–Sen slope estimates of sea surface temperature (SST), cloud fraction (CF), and chlorophyll concentration (CHL) and counts of LMEs with significant negative and positive slopes in the same parameters.

Category	Value	SST	CF	CHL
All	LMEs with negative trend	17	6	57
	Percentage	26%	9%	86%
	LMEs with positive trend	49	60	9
	Percentage	74%	91%	14%
Significant	LMEs with negative trend	0	1	40
	Percentage	0%	3%	100%
	LMEs with positive trend	23	29	0
	Percentage	100%	97%	0%

Fig. 7. Mean chlorophyll concentration (CHL) time series in all large marine ecosystems (LMEs) (*a*), LMEs with nonsignificant trends (*b*), and LMEs with significant trends (*c*). PC 1 of a principal components analysis of CHL time series in all LMEs (*d*), LMEs with nonsignificant trends (*e*), and LMEs with significant trends (*f*). [Colour online.]

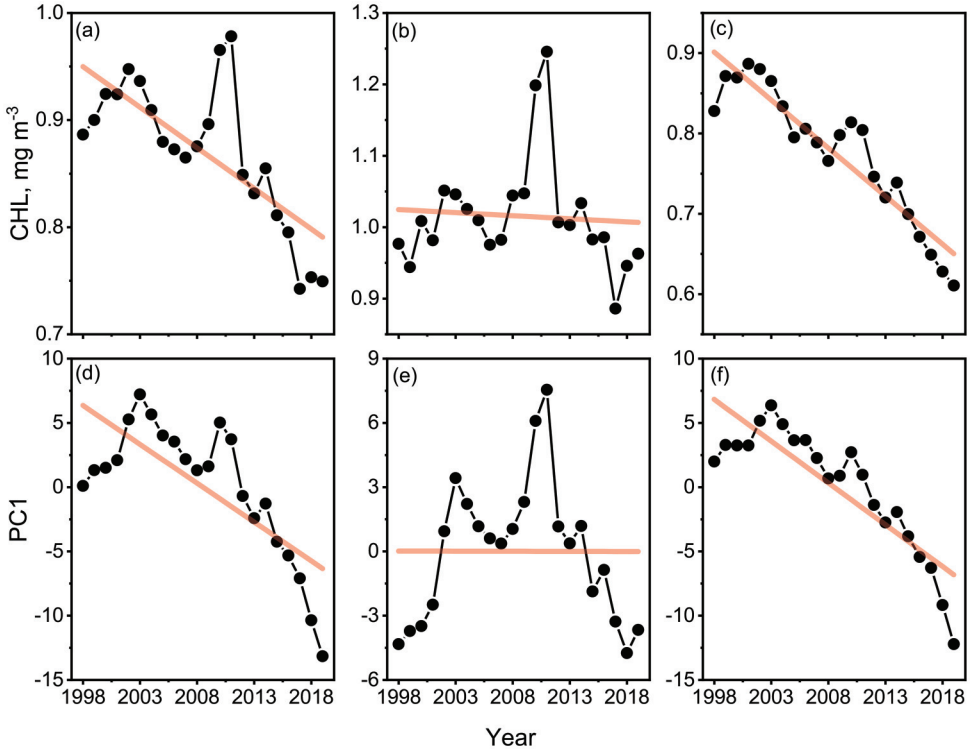

global data, 57 LMEs had negative CHL trends, representing 86% of the total. Of these trends, 40 were significant, all of which were negative trends. To provide further context for the change in CHL within LMEs, mean CHL for all LMEs is plotted in Fig. 7*a*, which suggests CHL has declined by 0.2 mg·m^{-3} over the period. In LMEs without significant change in CHL, concentrations were virtually unchanged over the study period (Fig. 7*b*). Finally, in LMEs with significant trends, CHL has declined nearly 0.3 mg·m^{-3} over the study period (Fig. 7*c*). The same trends were characterized with principal components (Figs. 7*d*–7*f*); since the first dimension of the PCA data reflects the means of the raw data, we can have greater confidence in the trends suggested by LME groupings.

Trend in PFT

The contribution of different PFTs, determined using the Moisan et al. (2017) method, changed whether inside or outside LMEs. The percent contribution of diatoms and dinoflagellates appears to have decreased at a greater rate within LMEs compared to trends at the global scale (Figs. 8*a*, 8*b*). Diatoms appear to have increased in parts of the Global Ocean outside LMEs. On the other hand, green algae, prymnesiophytes, and cyanobacteria appear to have increased within LMEs (Figs. 8*c*, 8*d*, 8*e*). The global distribution of the Theil–Sen slopes for each of these PFTs can be seen in Supplementary Figs. S2 through S6[1]. Trends within individual LMEs followed the same patterns of change indicated by the mean trends on global scales. The percent contribution of diatoms in 46 LMEs trended positive, which represents 70% of all LMEs (Table 4 and see Supplementary Table S2[1] for statistics for each LME). Of the diatom trends in LMEs, 35 were significant at $p < 0.1$, 33 of which were positive trends. Though not as strong a signal, 39 LMEs had positive trends in the contribution of dinoflagellates and the majority of significant trends were positive. In contrast, at least 70% of the LME trends for green algae, prymnesiophytes, and cyanobacteria were negative; and, of the significant trends, at least 90% were negative.

Trends in world fisheries

Though trends in catches and CPUE in global and LME fisheries differed, they were both consistent in suggesting that fishery resource biomass has not increased, and that the more likely interpretation would be biomass has declined. Catch appears to have decreased globally and within LMEs and increased outside LMEs; however, the differences in these trends were of low magnitude (Figs. 9*a*, 9*b*, 9*c*). Global and LME catches both declined over the study period at decadal rates of <0.001 and 1.0 10^6 t·decade^{-1}, respectively; however, neither trends were significant at any reasonable probability level (Table 5). The fisheries catch trend outside LMEs was weakly positive at 0.3 10^6 t·decade^{-1} and nonsignificant. Negative trends of catch within individual LMEs numbered slightly more than positive trends; 37 LMEs had negative trends, which represented 56% of the total (Supplementary Table S3[1]). Of these LME trends, 37 were significant at $p < 0.1$ and 57% were negative. Hence, the catch data suggest little change in biomass over the study period.

On the other hand, trends in CPUE were negative and highly significant for both global and inside and outside LMEs. The rate of decrease in CPUE ranged from approximately 0.39 to 0.53 t $\times$ 10^{-3} per unit of effort per decade, all of these trend estimates were significant. Negative trends in CPUE within individual LMEs numbered more than positive trends; 44 LMEs had negative trends, which represent 66% of the total. Of these LME trends, only 29 were significant at $p < 0.1$, probably owing to the short length of the time series and the high degree of autocorrelation of some of the data. However, 83% of the significant trends were negative. In contract to the catch data, the CPUE data suggests a marked decline in biomass over the study period.

Table 4. Counts of large marine ecosystems (LMEs) with negative and positive Theil–Sen slope estimates of percent contribution of diatoms (DIAT), dinoflagellates (DINO), green algae (GREEN), prymnesiophytes (PRYM), and cyanobacteria (CYAN) and counts of LMEs with significant negative and positive slopes in the same parameters.

Category	Value	DIAT	DINO	GREEN	PRYM	CYAN
All	LMEs with negative trend	46	39	20	20	18
	Percentage	70%	59%	30%	30%	27%
	LMEs with positive trend	20	27	46	46	48
	Percentage	30%	41%	70%	70%	73%
Significant	LMEs with negative trend	33	22	3	2	0
	Percentage	94%	76%	10%	6%	0%
	LMEs with positive trend	2	7	26	31	37
	Percentage	6%	24%	90%	94%	100%

Fig. 8. Mean of 1° Theil–Sen slope estimates of diatoms (*a*), dinoflagellates (*b*), green algae (*c*), prymnesiophytes (*d*), and cyanobacteria (*e*) as decadal rates over the globe (GLOBE), within large marine ecosystems (IN), and outside large marine ecosystems (OUT) for the period 1998–2019; error bars are 99% confidence intervals. [Colour online.]

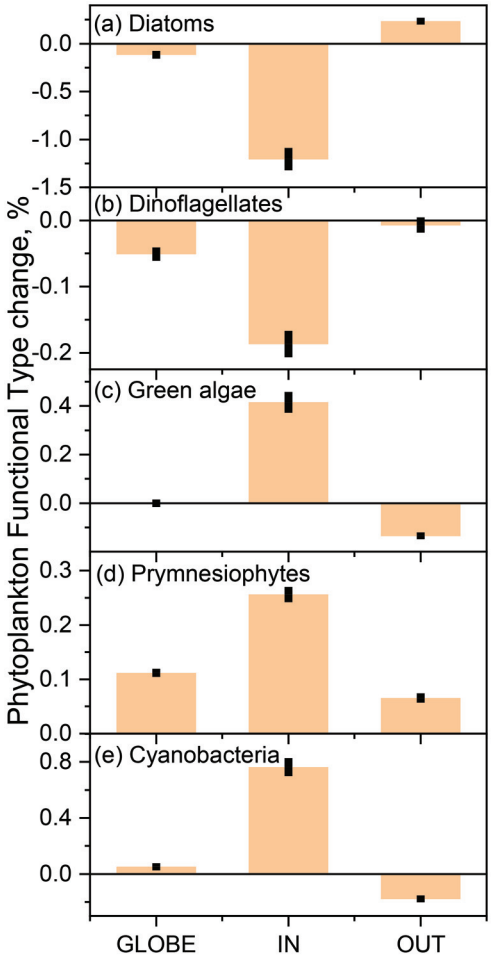

Discussion

We examined observational and remote sensing based global data sets and found evidence of differential change in physical and biological parameters between the global ocean and the LMEs comprising continental shelf seas. Global warming trends in the ocean surface layer were more intense in the LMEs than the global ocean, which has been accompanied by a reduction in solar radiation reaching these areas suggested by increasing cloud fraction trends. Both changes in temperature and cloud cover have the potential to reshape the timing and magnitude of phytoplankton blooms (La and Park 2016; Trombetta et al. 2019). The multi-sensor chlorophyll concentration data product suggests these physical changes may have differentially caused a stronger decline in phytoplankton biomass in LMEs compared to the global ocean, a result that suggests phytoplankton community structure within LMEs may have changed. Diatoms play an important role in ocean food webs (Harvey et al. 2019), and the reduction in the contribution of diatom taxa to phytoplankton communities could be a point of concern for food webs dynamics in LMEs. At face value, our estimates suggest that phytoplankton biomass has had a decadal rate of decline approaching 10% of the mean in LMEs as a whole. This decline, taken with the putative change in phytoplankton communities in LMEs, places our focus on the ability of these ecosystems to continue to support world food security (Link et al. 2020). We have shown that world catch corrected for nominal effort suggests a decline in upper trophic level productivity in the ocean and in particular in LMEs. There are many factors affecting resource species including exploitation and other anthropogenic effects; however, this decline in fisheries productivity is consistent with a decline in the productivity of lower trophic levels. We acknowledge that the satellite time series we used are relatively short (22 years) to support the confident identification of time series trends (Henson et al. 2016); however, we took a duplicative approach in constructing our trend test and we used conservative testing methods that applied corrections for autocorrelation. We also recognize the continued challenges in estimating chlorophyll concentration from remote sensing data given the differences between the estimates of CHL coming from different sensors and the drift in measurements from individual sensors over time (Yuan et al. 2020). In addition, we note that chlorophyll derived from remote sensing products presents a 2-dimensional view of 3-dimensional processes, which include mixed layer depth, light attenuation, and nutrient mixing from subsurface waters (Doney 2006). All of which underscores the importance of in situ high-resolution validation of chlorophyll, pigments, and remote sensing reflectance.

Climate-scale ocean modeling studies predict that accelerated warming of the oceans will alter the vertical structure of the upper water column by enhancing the density gradient at the base of the mixed layer (Capotondi et al. 2012). A modeling study aimed at understanding the impact of these changes on ocean ecosystems (Jang et al. 2011) suggests that primary production could be reduced by 11% to 40% due to decreased fluxes of nutrients into the mixed layer. Moreover, this study suggests that spring blooms could be initiated by as much as 13 days earlier. The projected increase in upper ocean temperatures should lead to earlier onset of phytoplankton blooms, but the anticipated decreased nutrient fluxes could counter this effect, as lower nutrient fluxes will likely slow the rate of bloom development. However, Somavilla et al. (2017), using in situ observations and ocean reanalysis data,

Fig. 9. Time series of catch and catch per unit effort (CPUE) in the global ocean (*a*), inside large marine ecosystems (*b*), and outside large marine ecosystems (*c*). [Colour online.]

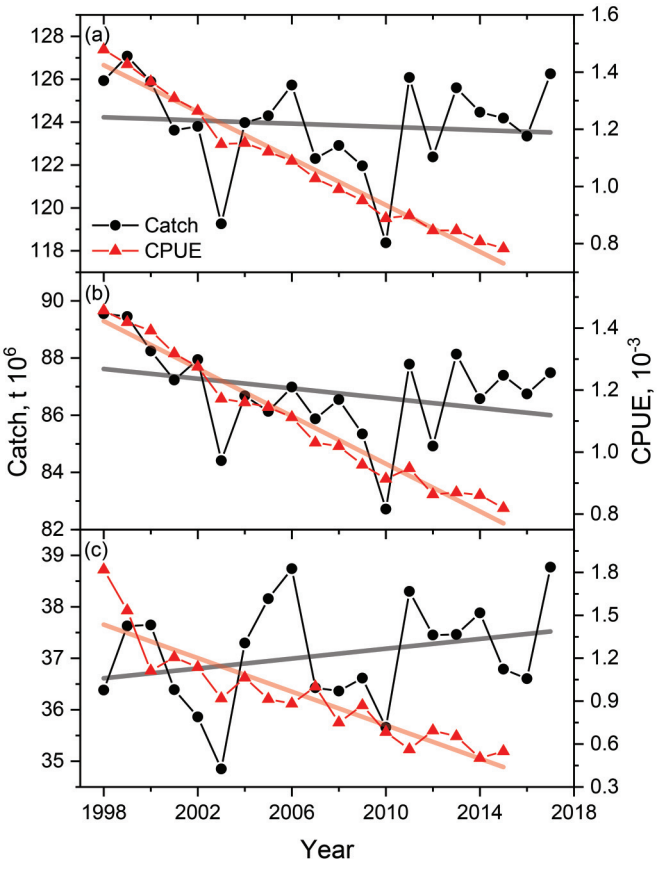

notes that while seasonal changes in the mixed layer depth force the observed seasonal evolution of the upper ocean ecosystem, changes in the mixed layer depth are not directly controlled by local sea surface temperatures. Rather, large-scale circulation processes influence the structure of the thermocline. Therefore, while SST levels have generally increased for most of the ocean, they found that mixed layer depths have not consistently shown coincident levels of shoaling. In a more contemporary analysis, Sallée et al. (2021) found that summertime mixed layer depths have deepened by approximately 3% per decade suggesting dramatic changes in the circulation dynamics of the upper layer of the global ocean.

Climate change has had interconnected impacts on the hydrosphere through changes in energy flow through the atmosphere. In addition to governing the way heat and kinetic energy is transferred to the ocean, the atmosphere affects the transmission of solar energy. Phytoplankton growth is dependent on the amount of PAR incident to the ocean surface, which can be disrupted by shading clouds. With increasing global temperatures in recent decades, the atmosphere is holding more water vapor and producing greater precipitation, especially along the coastal margins (Curtis 2019). Long-term change in cloud cover has not been uniform by area or formation; low altitude, tropically distributed clouds have generally decreased whereas more widely distributed convective clouds have generally increased over time (Mishra 2019). Moreover, clouds are not the only impediment to light transmission through the atmosphere, since it has been found that aerosols have also contributed to the general dimming effect seen globally since 2000 (Hatzianastassiou et al. 2020). Though anthropogenic forcing related to greenhouse gases has had an effect on the change in cloud distribution in time and space, decadal variability associated

Table 5. Theil–Sen slope estimates for catch (t, $\times 10^6$) and catch per unit effort (CPUE, $\times 10^{-3}$) globally and inside and outside large marine ecosystems.

Source	Global	Inside	Outside
Catch	0.000	–1.000	0.310
CPUE	**–0.410**	**–0.393**	**–0.532**

Note: Significant ($p < 0.01$) estimates shown in bold.

with large-scale climate processes like the Pacific Decadal Oscillation or Atlantic Multidecadal Oscillation also affects the distribution of clouds (Chen et al. 2019). Though phytoplankton can adapt to variability in subsurface light levels (Jyothibabu et al. 2018), cloud cover has been found to have important impacts on a range of ecological processes in addition to photosynthesis (Wilson and Jetz 2016). Furthermore, a reduction in solar radiation may also affect the phenology of phytoplankton blooms synergistically with other drivers of ecosystem change. Phytoplankton adapt their chlorophyll to carbon levels to optimize sunlight absorption and nutrient availability (Behrenfeld et al. 2016; Castellani and Edwards 2017). The larger impact seems to be a delay in the spring bloom due to reduced rates of phytoplankton growth. However, if reductions in light levels coincide with increased sea temperatures, which cause spring blooms to occur earlier, the opposing impacts from these two forcing factors should reduce the shift in the timing of the spring blooms.

We concentrated on the cause and effect between temperature, cloud fraction, and chlorophyll concentration; however, we are cognizant of the fact that many other factors control lower-level productivity. Basin boundary upwelling systems, which are some of the most productive marine ecosystems in the world, are primarily limited by the wind-driven supply of nutrients to the surface (Pauly and Christensen 1995). Some coastal ecosystems are affected by riverine nutrient inputs (Teixeira et al. 2018), a special case being coastal glacial runoff that provides nutrients like iron and silicic acid, but also actuates deep circulation that brings nitrate to the surface (Hopwood et al. 2018). Patterns of phytoplankton productivity may also be controlled by the ecology of their resting stages (Ellegaard and Ribeiro 2018) or grazing pressure (Anderson and Harvey 2019). Many large marine ecosystems will respond to climate change effects like increasing temperature and diminishing solar radiation in much the same way; however, it is easy to see where many LMEs may have exceptional and varied responses to climate change depending on physical setting of the ecosystem and biological factors that may be controlling phytoplankton growth.

Changes in the phytoplankton population composition are expected to occur as ocean temperatures rise due to climate change. It is expected that with increased stratification there will be decreased nutrient flux to the photic layer contributing to temperature-driven changes in phytoplankton population composition. Under a regime of diminished nutrients, phytoplankton that thrive in more nutrient-rich domains, such as diatoms and dinoflagellates, should become less dominant and replaced by other functional types such as small-celled prymnesiophytes and cyanobacteria, that often thrive under nutrient-poor conditions (Burson et al. 2018). Diatoms have historically been identified as being the highest quality food type within marine phytoplankton assemblages, due in part to their ability to store lipids (Yi et al. 2017). They also play an important role in Global Ocean biogeochemistry because of their need for silicate and iron and rapid sinking rates (Smetacek 2018). Interestingly, recent studies (Valenzuela et al. 2018) suggest that high pCO_2 environments favor marine diatom populations. Diatoms are the chief food source for marine copepods, which are the dominant link in marine food webs between phytoplankton and fish populations (Turner 2004). The suggested differential change in the contribution of diatoms between the Global Ocean and within LMEs should

provide sufficient rationale for further work on this important aspect of marine ecosystems.

The relationships between oceanographic conditions like temperature, phytoplankton, and the yield of resource species are challenging to understand, especially so under conditions associated with a changing climate. Increasingly, biotic communities reflect control that can be attributed to climate change rather than fishing pressure (Merillet et al. 2020). A reasonable expectation would be that higher trophic level species would suffer decreased growth and biomass with increasing temperature and declining primary production, noting that such biomass declines have been observed in some regions (Lotze et al. 2019; Hastings et al. 2020). However, other examples suggest an expansion of abundance and biomass in some ecosystems that have experienced changed climate conditions. For example, in temperate systems, changes in system organization, often referred to as "tropicalization", can result in expanded habitats that accompany an overall increase in biomass (Friedland et al. 2020). Similar expansion of species abundances have also occurred in boreal systems associated with poleward movements in species distribution (Spies et al. 2020), which has been attributed to reorganized biotic interactions in food webs. In these systems, generalist feeders move to higher latitudes and establish themselves, promoting greater food web connectivity in the ecosystem and facilitating energy transfer between pelagic and benthic habitats (Kortsch et al. 2015; Frainer et al. 2017). The newly established feeding interactions are considered novel since they are exploiting previously underutilized pathways of energy flow (Pecuchet et al. 2020). Such changes, while favoring the abundance of generalist species feeding on the benthic and pelagic pathways, also threaten benthic specialist species. The establishment of demersal/benthopelagic generalist species into previously unoccupied northern areas depends on benthic productivity (van Denderen et al. 2018; Petrik et al. 2019), which is not investigated in this study. However, temperate and boreal ecosystems may eventually become too saturated to realize biomass gains from food web diversification despite reductions in growth due to changes in temperature and primary production. Ensemble model projections predict declines in biomass at high trophic levels over the next century due to increasing temperature and decreasing primary production, the effect of which is concentrated or amplified (Lotze et al. 2019), resulting in a decrease in fisheries yield in the long-term.

Though any linkage between CHL and fishery yields within LMEs is not conclusively established with our analysis, the putative trend in LME CPUE is at least consistent with a reduction of lower trophic level productivity. The factors influencing catch on global or local scales are numerous and complex owing to not only ecosystem effects, but also due to social change and human requirements. However, it should be noted that global fishing intensity (effort) and efficiency, especially in the inshore LME areas, has been continuously increasing to compensate for declining catches (Bell et al. 2017; Rousseau et al. 2019). Given a steady state regime of lower trophic level productivity, there would be an expectation of increasing yields with increasing effort (Watson et al. 2013). Collectively, our observations suggest that the lower trophic level productivity of LMEs has been in decline (Chassot et al. 2010) and is limiting the productivity of upper trophic level species and their catches, as previous work would suggest (Stock et al. 2017). To emphasize the point, catches have not increased despite increasing effort, most likely because of the declines in system productivity. If some measure of decreasing LME fisheries production were related to contracting phytoplankton communities, the ramifications would be widespread and concerning.

Declaration of competing interest

The authors declare no competing interests.

Author contributions

The analyses in the paper were conceived and performed by Friedland, Moisan, Watson, and Rousseau. All authors contributed to the development and refinement of the text of the paper.

Data availability statement

Data sharing is not applicable to this article as no new data were created in this study. The data that support the findings of this study were derived from the following resources available in the public domain: Physical Sciences Laboratory website (https://psl.noaa.gov/data/gridded/data.noaa.oisst.v2.html); Hermes GlobColour website (http://hermes.acri.fr/). World catch data available for public download (http://dx.doi.org/10.4226/77/5a65572655f73; http://data.imas.utas.edu.au/portal/search?uuid=ff1274e1-c0ab-411b-a8a2-5a12eb27f2c0). Global fishing effort data (dx.doi.org/10.25959/5f5aea5441751).

Acknowledgements

We thank S. Large for comments on an early draft of the paper. Funding for J. Moisan was provided for by the NASA Ecosystem Forecasting Program, The Gordon and Betty Moore Foundation under Grant Number 3292, and the NASA Applied Information Systems Technology Program under NNH18ZDA001N-AIST. A. Maureaud conducted the work within the Centre for Ocean Life, a Villum Kann Rasmussen Center of Excellence supported by the Villum Foundation. Funding for D. Brady participation provided by NSF grant No. 1849227 and National Sea Grant award NA19OAR4170395.

References

Anderson, S.R., and Harvey, E.L. 2019. Seasonal variability and drivers of microzooplankton grazing and phytoplankton growth in a subtropical estuary. Front. Mar. Sci. **6**: 174. doi:10.3389/fmars.2019.00174.

Asch, R.G., Stock, C.A., and Sarmiento, J.L. 2019. Climate change impacts on mismatches between phytoplankton blooms and fish spawning phenology. Global Change Biol. **25**(8): 2544–2559. doi:10.1111/gcb.14650.

Batt, R.D., Morley, J.W., Selden, R.L., Tingley, M.W., and Pinsky, M.L. 2017. Gradual changes in range size accompany long-term trends in species richness. Ecol. Lett. **20**(9): 1148–1157. doi:10.1111/ele.12812. PMID:28699209.

Behrenfeld, M.J., O'Malley, R.T., Boss, E.S., Westberry, T.K., Graff, J.R., Halsey, K.H., et al. 2016. Revaluating ocean warming impacts on global phytoplankton. Nat. Clim. Change, **6**(3): 323–330. doi:10.1038/nclimate2838.

Bell, J.D., Watson, R.A., and Ye, Y. 2017. Global fishing capacity and fishing effort from 1950 to 2012. Fish Fish. **18**(3): 489–505. doi:10.1111/faf.12187.

Burrows, M.T., Bates, A.E., Costello, M.J., Edwards, M., Edgar, G.J., Fox, C.J., et al. 2019. Ocean community warming responses explained by thermal affinities and temperature gradients. Nat. Clim. Change, **9**(12): 959–963. doi:10.1038/s41558-019-0631-5.

Burson, A., Stomp, M., Greenwell, E., Grosse, J., and Huisman, J. 2018. Competition for nutrients and light: testing advances in resource competition with a natural phytoplankton community. Ecology, **99**(5): 1108–1118. doi:10.1002/ecy.2187. PMID:29453803.

Capotondi, A., Alexander, M.A., Bond, N.A., Curchitser, E.N., and Scott, J.D. 2012. Enhanced upper ocean stratification with climate change in the CMIP3 models. J. Geophys. Res.-Oceans. **117**. doi:10.1029/2011jc007409.

Castellani, C., and Edwards, M. 2017. Marine plankton: a practical guide to ecology, methodology, and taxonomy. Oxford University Press.

Chassot, E., Bonhommeau, S., Dulvy, N.K., Melin, F., Watson, R., Gascuel, D., and Le Pape, O. 2010. Global marine primary production constrains fisheries catches. Ecol Lett. **13**(4): 495–505. doi:10.1111/j.1461-0248.2010.01443.x. PMID:20141525.

Chen, Y.-J., Hwang, Y.-T., Zelinka, M.D., and Zhou, C. 2019. Distinct patterns of cloud changes associated with decadal variability and their contribution to observed cloud cover trends. J. Climate. **32**(21): 7281–7301. doi:10.1175/JCLI-D-18-0443.1.

Cheng, L., Abraham, J., Hausfather, Z., and Trenberth, K.E. 2019. How fast are the oceans warming? Science, **363**(6431): 128–129. doi:10.1126/science.aav7619. PMID:30630919.

Christensen, V., Walters, C.J., Ahrens, R.N.M., Alder, J., Buszowski, J., and Christensen, L.B., 2008. Models of the world's large marine ecosystems. Technical Series. Intergovernmental Oceanographic Commission = Série technique. Available from http://www.vliz.be/en/imis?refid=129497 [accessed 24 June 2020].

Costanza, R., de Groot, R., Sutton, P., van der Ploeg, S., Anderson, S.J., Kubiszewski, I., et al. 2014. Changes in the global value of ecosystem services. Global Environ. Change, **26**: 152–158. doi:10.1016/j.gloenvcha.2014.04.002.
Curtis, S. 2019. Means and long-term trends of global coastal zone precipitation. Sci. Rep. **9**: 5401. doi:10.1038/s41598-019-41878-8. PMID:30931984.
Dantas, D.D.F., Caliman, A., Guariento, R.D., Angelini, R., Carneiro, L.S., Lima, S.M.Q., et al. 2019. Climate effects on fish body size – trophic position relationship depend on ecosystem type. Ecography, **42**(9): 1579–1586. doi:10.1111/ecog.04307.
Doney, S.C. 2006. Plankton in a warmer world. Nature, **444**(7120): 695–696. doi:10.1038/444695a. PMID:17151650.
Durant, J.M., Molinero, J.C., Ottersen, G., Reygondeau, G., Stige, L.C., and Langangen, O. 2019. Contrasting effects of rising temperatures on trophic interactions in marine ecosystems. Sci. Rep. **9**: 15213. doi:10.1038/s41598-019-51607-w.
Dutkiewicz, S., Hickman, A.E., Jahn, O., Henson, S., Beaulieu, C., and Monier, E. 2019. Ocean colour signature of climate change. Nat. Commun. **10**: 578. doi:10.1038/s41467-019-08457-x.
Ellegaard, M., and Ribeiro, S. 2018. The long-term persistence of phytoplankton resting stages in aquatic 'seed banks'. Biol. Rev. **93**(1): 166–183. doi:10.1086/698086, doi:10.1111/brv.12338. PMID:28474820.
Frainer, A., Primicerio, R., Kortsch, S., Aune, M., Dolgov, A.V., Fossheim, M., and Aschan, M.M. 2017. Climate-driven changes in functional biogeography of Arctic marine fish communities. Proc. Natl. Acad. Sci. U.S.A. **114** (46): 12202–12207. doi:10.1073/pnas.1706080114. PMID:29087943.
Friedland, K.D., Ahrenholz, D.W., and Haas, L.W. 2005. Viable gut passage of cyanobacteria through the filter-feeding fish Atlantic menhaden, *Brevoortia tyrannus*. J. Plankton Res. **27**(7): 715–718. doi:10.1093/plankt/fbi036.
Friedland, K.D., Mouw, C.B., Asch, R.G., Ferreira, A.S.A., Henson, S., Hyde, K.J.W., et al. 2018. Phenology and time series trends of the dominant seasonal phytoplankton bloom across global scales. Global Ecol. Biogeogr. **27**(5): 551–569. doi:10.1111/geb.12717.
Friedland, K.D., Langan, J.A., Large, S.I., Selden, R.L., Link, J.S., Watson, R.A., and Collie, J.S. 2020. Changes in higher trophic level productivity, diversity and niche space in a rapidly warming continental shelf ecosystem. Sci. Total Environ. **704**: 135270. doi:10.1016/j.scitotenv.2019.135270. PMID:31818590.
Groom, S., Sathyendranath, S., Ban, Y., Bernard, S., Brewin, R., Brotas, V., et al. 2019. Satellite ocean colour: current status and future perspective. Front Mar Sci. **6**: 485. doi:10.3389/fmars.2019.00485.
Halpern, B.S., Selkoe, K.A., Micheli, F., and Kappel, C.V. 2007. Evaluating and ranking the vulnerability of global marine ecosystems to anthropogenic threats. Conserv. Biol. **21**(5): 1301–1315. doi:10.1111/j.1523-1739.2007.00752.x. PMID:17883495.
Harvey, B.P., Agostini, S., Kon, K., Wada, S., and Hall-Spencer, J.M. 2019. Diatoms dominate and alter marine food-webs when CO_2 rises. Diversity, **11**(12): 242. doi:10.3390/d11120242.
Hastings, R.A., Rutterford, L.A., Freer, J.J., Collins, R.A., Simpson, S.D., and Genner, M.J. 2020. Climate change drives poleward increases and equatorward declines in marine species. Curr. Biol. **30**(8): 1572–1577 e2. doi:10.1016/j.cub.2020.02.043. PMID:32220327.
Hatzianastassiou, N., Ioannidis, E., Korras-Carraca, M.-B., Gavrouzou, M., Papadimas, C.D., Matsoukas, C., et al. 2020. Global dimming and brightening features during the first decade of the 21st Century. Atmosphere, **11**(3): 308. doi:10.3390/atmos11030308.
Henson, S., Cole, H., Beaulieu, C., and Yool, A. 2013. The impact of global warming on seasonality of ocean primary production. Biogeosciences, **10**(6): 4357–4369. doi:10.5194/bg-10-4357-2013.
Henson, S.A., Beaulieu, C., and Lampitt, R. 2016. Observing climate change trends in ocean biogeochemistry: when and where. Global Change Biol. **22**(4): 1561–1571. doi:10.1111/gcb.13152.
Hirata, T., Hardman-Mountford, N.J., Brewin, R.J.W., Aiken, J., Barlow, R., Suzuki, K., et al. 2011. Synoptic relationships between surface chlorophyll-*a* and diagnostic pigments specific to phytoplankton functional types. Biogeosciences, **8**(2): 311–327. doi:10.5194/bg-8-311-2011.
Hopwood, M.J., Carroll, D., Browning, T.J., Meire, L., Mortensen, J., Krisch, S., and Achterberg, E.P. 2018. Non-linear response of summertime marine productivity to increased meltwater discharge around Greenland. Nat. Commun. **9**(1): 3256. doi:10.1038/s41467-018-05488-8. PMID:30108210.
Howarth, L.M., Roberts, C.M., Thurstan, R.H., and Stewart, B.D. 2014. The unintended consequences of simplifying the sea: making the case for complexity. Fish Fish. **15**(4): 690–711. doi:10.1111/faf.12041.
Huxel, G.R., and McCann, K. 1998. Food web stability: The influence of trophic flows across habitats. Am. Nat. **152**(3): 460–469. doi:10.1086/286182. PMID:18811452.
Jang, C.J., Park, J., Park, T., and Yoo, S. 2011. Response of the ocean mixed layer depth to global warming and its impact on primary production: a case for the North Pacific Ocean. ICES J. Mar. Sci. **68**(6): 996–1007. doi:10.1093/icesjms/fsr064.
Jeffrey, S.W., Wright, S.W., and Zapata, M. 2011. Microalgal classes and their signature pigments. *In* Phytoplankton pigments: characterization, chemotaxonomy and applications in oceanography. *Edited by* C.A. Llewellyn, E.S. Egeland, G. Johnsen, and S. Roy. Cambridge University Press, Cambridge. pp. 3–77. doi:10.1017/CBO9780511732263.004.
Joy-Warren, H.L., Dijken, G.L.V., Alderkamp, A.-C., Leventer, A., Lewis, K.M., Selz, V., et al. 2019. Light is the primary driver of early season phytoplankton production along the western Antarctic Peninsula. J. Geophys. Res. Oceans, **124**(11): 7375–7399. doi:10.1029/2019JC015295.
Jyothibabu, R., Arunpandi, N., Jagadeesan, L., Karnan, C., Lallu, K.R., and Vinayachandran, P.N. 2018. Response of phytoplankton to heavy cloud cover and turbidity in the northern Bay of Bengal. Sci. Rep. **8**(1): 1–15. doi:10.1038/s41598-017-17765-5, doi:10.1038/s41598-018-33214-3. PMID:29311619.
Kortsch, S., Primicerio, R., Fossheim, M., Dolgov, A.V., and Aschan, M. 2015. Climate change alters the structure of arctic marine food webs due to poleward shifts of boreal generalists. Proc. R. Soc. B Biol. Sci. **282**(1814): 31–39. doi:10.1098/rspb.2015.1546.
Kramer, S.J., and Siegel, D.A. 2019. How can phytoplankton pigments be best used to characterize surface ocean phytoplankton groups for ocean color remote sensing algorithms? J. Geophys. Res. Oceans, **124**(11): 7557–7574. doi:10.1029/2019JC015604. PMID:32140375.
La, H.S., and Park, K. 2016. The Evident Role of Clouds on Phytoplankton Abundance in Antarctic Coastal Polynyas. Terrest. Atmos. Ocean. Sci. **27**: 293–301. doi:10.3319/TAO.2015.11.30.01(Oc).
Lawson, C.L., and Hanson, R.J. 1995. Solving least squares problems. Society for Industrial and Applied Mathematics. doi:10.1137/1.9781611971217.
Link, J.S., Watson, R.A., Pranovi, F., and Libralato, S. 2020. Comparative production of fisheries yields and ecosystem overfishing in African large marine ecosystems. Environ. Dev. **36**: 100529. doi:10.1016/j.envdev.2020.100529.
Lotze, H.K., Tittensor, D.P., Bryndum-Buchholz, A., Eddy, T.D., Cheung, W. W.L., Galbraith, E.D., et al. 2019. Global ensemble projections reveal trophic amplification of ocean biomass declines with climate change. Proc. Natl. Acad. Sci. U.S.A. **116**(26): 12907–12912. doi:10.1073/pnas.1900194116. PMID:31186360.
Mann, H.B. 1945. Nonparametric tests against trend. Econometrica, **13**: 245–259. doi:10.2307/1907187.
Maritorena, S., d'Andon, O.H.F., Mangin, A., and Siegel, D.A. 2010. Merged satellite ocean color data products using a bio-optical model: characteristics, benefits and issues. Remote Sens. Environ. **114**(8): 1791–1804. doi:10.1016/j.rse.2010.04.002.
Merillet, L., Kopp, D., Robert, M., Mouchet, M., and Pavoine, S. 2020. Environment outweighs the effects of fishing in regulating demersal community structure in an exploited marine ecosystem. Global Change Biol. **26**: 2106–2119. doi:10.1111/gcb.14969.
Mishra, A.K. 2019. Investigating changes in cloud cover using the long-term record of precipitation extremes. Meteorol. Appl. **26**(1): 108–116. doi:10.1002/met.1745.
Moisan, T.A., Rufty, K.M., Moisan, J.R., and Linkswiler, M.A. 2017. Satellite observations of phytoplankton functional type spatial distributions, phenology, diversity, and ecotones. Front. Mar. Sci. **4**: 189. doi:10.3389/fmars.2017.00189.
Paerl, H.W. 2018. Mitigating toxic planktonic cyanobacterial blooms in aquatic ecosystems facing increasing anthropogenic and climatic pressures. Toxins, **10**(2): 76. doi:10.3390/toxins10020076.
Pauly, D., and Christensen, V. 1995. Primary production required to sustain global fisheries. Nature, **374**(6519): 255–257. doi:10.1038/374255a0.
Pecuchet, L., Blanchet, M.-A., Frainer, A., Husson, B., Jørgensen, L.L., Kortsch, S., and Primicerio, R. 2020. Novel feeding interactions amplify the impact of species redistribution on an Arctic food web. Global Change Biol. **26**(9): 4894–4906. doi:10.1111/gcb.15196.
Petrik, C.M., Stock, C.A., Andersen, K.H., van Denderen, P.D., and Watson, J.R. 2019. Bottom-up drivers of global patterns of demersal, forage, and pelagic fishes. Prog. Oceanogr. **176**: 102124. doi:10.1016/j.pocean.2019.102124.
Press, W.H., Flannery, B.P., Teukolsky, S.A., Vetterling, W.T., and Gould, H. 1987. Numerical recipes, the art of scientific computing. Am. J. Phys. **55**(1): 90–91. doi:10.1119/1.14981.
Reynolds, R.W., Smith, T.M., Liu, C., Chelton, D.B., Casey, K.S., and Schlax, M.G. 2007. Daily high-resolution-blended analyses for sea surface temperature. J. Clim. **20**(22): 5473–5496. doi:10.1175/2007JCLI1824.1.
Rousseau, Y., Watson, R.A., Blanchard, J.L., and Fulton, E.A. 2019. Evolution of global marine fishing fleets and the response of fished resources. Proc. Natl. Acad. Sci. U.S.A. **116**: 12238–12243. doi:10.1073/pnas.1820344116. PMID:31138680.
Roxy, M.K., Modi, A., Murtugudde, R., Valsala, V., Panickal, S., Kumar, S.P., et al. 2016. A reduction in marine primary productivity driven by rapid warming over the tropical Indian Ocean. Geophys. Res. Lett. **43**(2): 826–833. doi:10.1002/2015gl066979. doi:10.1002/2015GL066979.
Sallée, J.-B., Pellichero, V., Akhoudas, C., Pauthenet, E., Vignes, L., Schmidtko, S., et al. 2021. Summertime increases in upper-ocean stratification and mixed-layer depth. Nature, **591**(7851): 592–598. doi:10.1038/s41586-021-03303-x. PMID:33762764.
Salo, T., Mattila, J., and Ekl?F, J. 2020. Long-term warming affects ecosystem functioning through species turnover and intraspecific trait variation. Oikos, **129**(2): 283–295. doi:10.1111/oik.06698.
Schiller, L., Bailey, M., Jacquet, J., and Sala, E. 2018. High seas fisheries play a negligible role in addressing global food security. Sci Adv. **4**(8): eaat8351. doi:10.1126/sciadv.aat8351.
Shackell, N.L., Bundy, A., Nye, J.A., and Link, J.S. 2012. Common large-scale responses to climate and fishing across Northwest Atlantic ecosystems. ICES J. Mar. Sci. **69**(2): 151–162. doi:10.1093/icesjms/fsr195.
Sherman, K. 1991. The large marine ecosystem concept: research and management strategy for living marine resources. Ecol. Appl. **1**(4): 349–360. doi:10.2307/1941896. PMID:27755673.

Sherman, K., and Duda, A.M. 1999. Large marine ecosystems: An emerging paradigm for fishery sustainability. Fisheries, **24**(12): 15–26. doi:10.1577/1548-8446(1999)024<0015:LME>2.0.CO;2.

Smetacek, V. 2018. Seeing is believing: diatoms and the ocean carbon cycle revisited. Protist, **169**(6): 791–802. doi:10.1016/j.protis.2018.08.004. PMID:30342384.

Somavilla, R., Gonzalez-Pola, C., and Fernandez-Diaz, J. 2017. The warmer the ocean surface, the shallower the mixed layer. How much of this is true? J. Geophys. Res. Oceans, **122**(9): 7698–7716. doi:10.1002/2017JC013125. PMID:29201584.

Spies, I., Gruenthal, K.M., Drinan, D.P., Hollowed, A.B., Stevenson, D.E., Tarpey, C.M., and Hauser, L. 2020. Genetic evidence of a northward range expansion in the eastern Bering Sea stock of Pacific cod. Evol. Appl. **13**(2): 362–375. doi:10.1111/eva.12874. PMID:31993082.

Stock, C.A., John, J.G., Rykaczewski, R.R., Asch, R.G., Cheung, W.W.L., Dunne, J.P., et al. 2017. Reconciling fisheries catch and ocean productivity. Proc. Natl. Acad. Sci. U.S.A. **114**(8): E1441–E1449. doi:10.1073/pnas.1610238114. PMID:28115722.

Strom, S.L., Macri, E.L., and Fredrickson, K.A. 2010. Light limitation of summer primary production in the coastal Gulf of Alaska: physiological and environmental causes. Mar. Ecol. Prog. Ser. **402**: 45–57. doi:10.3354/meps08456.

Teixeira, I.G., Arbones, B., Froján, M., Nieto-Cid, M., Álvarez-Salgado, X.A., Castro, C.G., et al. 2018. Response of phytoplankton to enhanced atmospheric and riverine nutrient inputs in a coastal upwelling embayment. Estuar. Coast. Shelf Sci. **210**: 132–141. doi:10.1016/j.ecss.2018.06.005.

Trombetta, T., Vidussi, F., Mas, S., Parin, D., Simier, M., and Mostajir, B. 2019. Water temperature drives phytoplankton blooms in coastal waters. PLoS ONE, **14**(4): e0214933. doi:10.1371/journal.pone.0214933. PMID:30951553.

Turner, J.T. 2004. The importance of small planktonic copepods and their roles in pelagic marine food webs. Zool. Stud. **43**: 255–266.

Uitz, J., Claustre, H., Morel, A., and Hooker, S.B. 2006. Vertical distribution of phytoplankton communities in open ocean: An assessment based on surface chlorophyll. J. Geophys. Res. **111**(C8). doi:10.1029/2005JC003207.

Ullah, H., Nagelkerken, I., Goldenberg, S.U., and Fordham, D.A. 2018. Climate change could drive marine food web collapse through altered trophic flows and cyanobacterial proliferation. PLoS Biol. **16**(1): e2003446. doi:10.1371/journal.pbio.2003446. PMID:29315309.

Valenzuela, J.J., López García de Lomana, A., Lee, A., Armbrust, E.V., Orellana, M.V., and Baliga, N.S. 2018. Ocean acidification conditions increase resilience of marine diatoms. Nat. Commun. **9**(1): 2328. doi:10.1038/s41467-018-04742-3. PMID:29899534.

van Denderen, P.D., Lindegren, M., MacKenzie, B.R., Watson, R.A., and Andersen, K.H. 2018. Global patterns in marine predatory fish. Nat. Ecol. Evol. **2**(1): 65–70. doi:10.1038/s41559-017-0388-z. PMID:29180711.

Watson, R.A., and Tidd, A. 2018. Mapping nearly a century and a half of global marine fishing: 1869–2015. Mar. Pol. **93**: 171–177. doi:10.1016/j.marpol.2018.04.023.

Watson, R.A., Cheung, W.W.L., Anticamara, J.A., Sumaila, R.U., Zeller, D., and Pauly, D. 2013. Global marine yield halved as fishing intensity redoubles. Fish Fish, **14**(4): 493–503. doi:10.1111/j.1467-2979.2012.00483.x.

Wilson, A.M., and Jetz, W. 2016. Remotely sensed high-resolution global cloud dynamics for predicting ecosystem and biodiversity distributions. PLOS Biol. **14**(3): e1002415. doi:10.1371/journal.pbio.1002415. PMID:27031693.

Wirtz, K.W. 2012. Who is eating whom? Morphology and feeding type determine the size relation between planktonic predators and their ideal prey. Mar. Ecol. Prog. Ser. **445**: 1–12. doi:10.3354/meps09502.

Yamaguchi, R., and Suga, T. 2019. Trend and variability in global upper-ocean stratification since the 1960s. J. Geophys. Res. Oceans, **124**: 8933–8948. doi:10.1029/2019jc015439.

Yi, Z., Xu, M., Di, X., Brynjolfsson, S., and Fu, W. 2017. Exploring Valuable Lipids in Diatoms. Front. Mar. Sci. **4**: 17. doi:10.3389/fmars.2017.00017.

Yuan, Q., Shen, H., Li, T., Li, Z., Li, S., Jiang, Y., et al. 2020. Deep learning in environmental remote sensing: achievements and challenges. Rem. Sens. Environ. **241**: 111716. doi:10.1016/j.rse.2020.111716.

Yue, S., Pilon, P., Phinney, B., and Cavadias, G. 2002. The influence of autocorrelation on the ability to detect trend in hydrological series. Hydrol. Process. **16**(9): 1807–1829. doi:10.1002/hyp.1095.